Electron holography of biased semiconductor devices

A C Twitchett, R E Dunin-Borkowski and P A Midgley

Department of Materials Science and Metallurgy, University of Cambridge, Pembroke Street, Cambridge, CB2 3QZ, UK

ABSTRACT: Off-axis and in-line electron holography have been used to examine a Si *p-n* junction under applied electrical bias. The experiments reveal the internal and external electrostatic potential distribution in the device. A quantitative analysis of the results was carried out using simulations, allowing a best-fitting model for the internal electrostatic potential distribution to be determined. The two complementary holographic techniques for the examination of semiconductor device structures reveal a layered electrostatic potential structure.

1. INTRODUCTION

Electron holography can be used to obtain both the phase and the amplitude of an electron wave that has passed through a TEM (transmission electron microscope) sample. When examining a semiconductor device structure, the phase image can reveal information about the electrostatic potential distribution in the sample. Off-axis electron holography has been used successfully to generate two-dimensional maps of phase modulations arising from a TEM membrane containing a semiconductor device (Rau et al 1999). However, a quantitative interpretation of the measured phase is complicated by many problems, which include the effects of sample preparation (e.g. strain, local thickness variations, surface damage) and charging of the TEM sample in the electron beam. The application of an electrical bias to a semiconductor device in the electron microscope allows some of these problems to be overcome by altering the electrical properties of the membrane whilst leaving several unwanted contributions to the measured phase unchanged.

In-line electron holography can also be used to examine the electrostatic potential across important features such as a *p-n* junction. The acquisition of an extended defocus series of bright field images of a sample containing a rapid variation in potential can be used to provide improved information complimentary to off-axis electron holography data. Although in-line and off-axis electron holography are both sensitive to the electrostatic potential, a discrepancy may arise between results obtained using the two techniques, both due to the relative insensitivity of Fresnel imaging to low spatial frequency variations in electrostatic potential and due to the presence of diffuse scattering (e.g. phonon) contributions to Fresnel contrast even if the images are energy filtered.

2. EXPERIMENTAL DETAILS

A *p-n* junction comprising a 2.5-μm-thick 5×10^{18} cm^{-3} B-doped (*p*-type) layer grown epitaxially on a 5×10^{18} cm^{-3} Sb-doped (*n*-type) substrate was prepared for TEM examination using focused ion beam (FIB) milling. Two sample geometries were prepared: (i) for unbiased experiments, standard trench milling was used to prepare an electron transparent window containing parallel-sided membranes of three different thickness; (ii) for biasing experiments, a combined cleaving and FIB milling method was used to prepare a single membrane of uniform thickness (Twitchett et al 2002). For both geometries, FIB milling was used to provide an area of vacuum close to the area of interest, thus optimising the sample geometry for off-axis electron holography. The crystalline thickness of each membrane was determined using convergent beam electron diffraction (CBED), and the total sample thickness (amorphous and crystalline) was measured in units of inelastic mean free path from the reconstructed off-axis amplitude image (Gajdardziska-Josifovska and McCartney 1994).

2.1 Off-axis electron holography

Off-axis electron holograms were acquired on a Philips CM300 field-emission TEM, which was operated in Lorentz mode and equipped with a Gatan GIF 2000, using a biprism voltage of between 80 and 100 V. Holograms were also acquired using a two-contact biasing holder to apply a reverse bias of between 0 and 3 V across the junction. Phase and amplitude images were reconstructed using library programs written in the Semper image processing language (Saxton et al 1979). Reference holograms were acquired immediately after acquiring holograms of the sample in order to remove distortions associated with the imaging and recording system. Holograms of biased samples were reconstructed both using a standard (empty) reference hologram and also using the 'zero bias' hologram. The latter procedure allows a 'differential' phase image to be obtained, revealing only the change in electrostatic potential arising from the change in electrical bias. Fig. 1(a) shows a reconstructed phase image acquired from an unbiased sample. Line profiles across the junction, projected along the junction over a distance of 116 nm, are shown for three sample thicknesses in Fig. 1(b). The extracted line profiles can be used to obtain quantitative information about the junction by relating the measured phase change across the junction, $\Delta\varphi$, to the built-in voltage, V_{bi} using the relation $\Delta\varphi = C_E\, V_{bi}\, t_{el}$ where t_{el} is the electrically active thickness of the TEM sample and C_E is a microscope-determined constant.

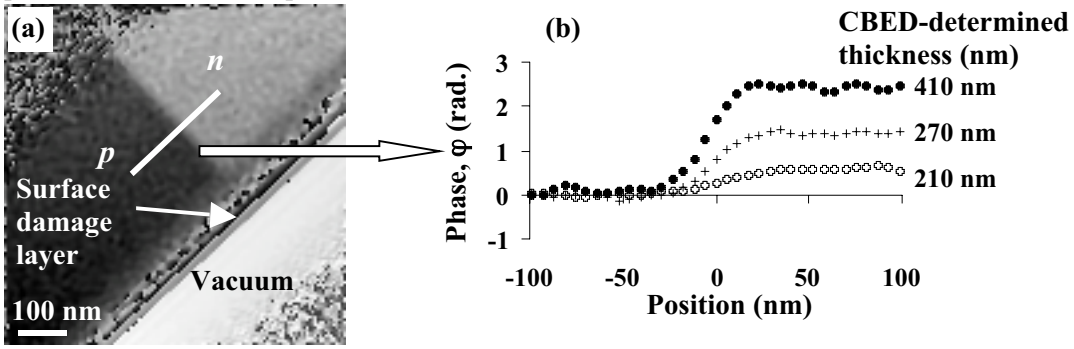

Fig. 1: (a) Reconstructed phase image of an unbiased FIB-prepared sample showing a damage layer resulting from sample preparation. (b) Phase profiles across the junction obtained from three different sample thicknesses, without an applied electrical bias.

2.2 In-line electron holography

Fresnel defocus series of both unbiased and reverse biased (0, 1, 2 and 3 V) samples were acquired in Lorentz mode using a defocus step size of 875 μm and a nominal magnification of 380×. Line profiles were obtained by averaging the contrast along the junction over a distance of 200 nm. These profiles were normalised by dividing by the background intensity for comparison with simulations. Fig. 2 shows a typical defocus series acquired from an unbiased membrane of crystalline thickness 410 nm.

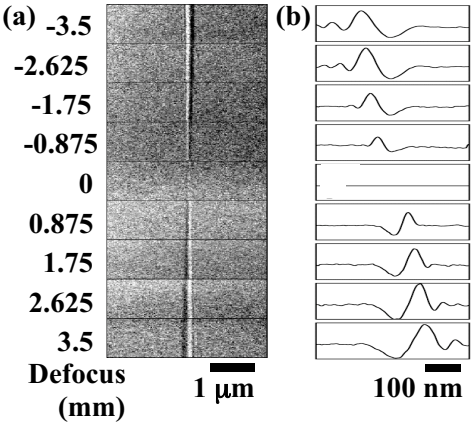

Fig. 2: (a) Experimental Fresnel defocus series of a *p*-*n* junction in an unbiased FIB-prepared Si membrane of crystalline thickness 410 nm. (b) The corresponding intensity profiles projected along the *p*-*n* junction. (Note the different horizontal scales in the two columns.)

2.3 Comparisons with simulations

Although Fresnel contrast images cannot be interpreted directly, a quantitative analysis of the data can be achieved through comparisons with image simulations. In the present study, a phase grating approximation was used to simulate the Fresnel contrast expected from a range of different potential profiles across a *p-n* junction. Three different models were examined for the potential variation in the TEM membrane: (i) an ideal abrupt *p-n* junction, (ii) an empirical equation for the charge density based on a smoothed *p-n* junction charge density profile and (iii) an abrupt model for the *p-n* junction, but with a varying depletion width which increased close to the sample surfaces. The parameters describing the sample potential were iterated using a Simplex algorithm until a best fit between simulations and the experimental data was obtained.

Phase profiles obtained using off-axis electron holography can, in contrast, be interpreted directly. However, experimental noise can prevent the calculation of the underlying charge density distribution. Using simulations similar to those described above, best fits were obtained to measured phase profiles. Charge density profiles were then inferred from the best-fitting simulations rather than from the original experimental data.

3. RESULTS AND DISCUSSION

Model (iii) described above consistently provided the optimal fit to the experimental results. Fig. 3(a) shows the fitted phase step across the *p-n* junction as a function of applied bias obtained from the off-axis electron holography results, with measurements obtained using both a standard reference hologram, and the zero-volt bias normalised image. From the linearity in the data, it can be inferred that the electrically active thickness is not changing with electrical bias, and the gradient can be used to obtain a value for the electrically active thickness, t_{el} of 330 nm. When compared to the crystalline thickness of 390 nm, this indicates the presence of 60 nm of crystalline, electrically 'dead' material presumably on the surfaces of the membrane. The intercept with the *y*-axis allows a value of 0.9 ± 0.05 V to be calculated for the built-in voltage, V_{bi}. These calculations assume that the external electrostatic potential does not contribute significantly to the measured phase change. Fig. 3(b) shows an amplified reconstructed phase image obtained at 3V reverse bias, normalised using the zero-volt bias hologram. The vacuum region is flat indicating that the external electrostatic potential is negligible and that the sample surface is an equipotential,

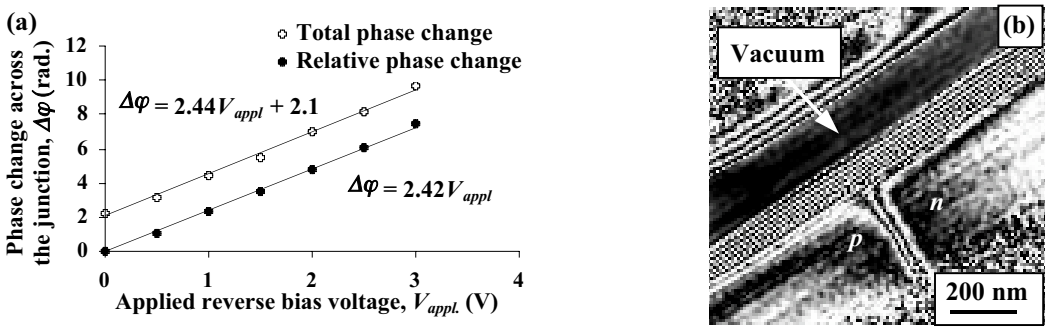

Fig. 3: (a) Phase change across the *p-n* junction plotted against applied voltage for phase images reconstructed using a vacuum reference hologram (total phase change), and using a zero bias hologram as a reference hologram (relative phase change). (b) Four times phase amplified image acquired using 3V reverse bias, reconstructed using the zero volt bias image as a reference hologram. The vacuum region does not show any phase variation confirming the absence of external electrostatic fringing fields outside FIB-prepared membranes.

A comparison of the Fresnel and off-axis holography results revealed a discrepancy. The contrast variation present in the Fresnel data was too small to be consistent with the results obtained by applying off-axis electron holography to the same sample. This low contrast could arise from the presence of an additional, uniform background intensity, perhaps from phonon scattering, which is not present in the off-axis data due to the difference in energy filtering between the two techniques. The Fresnel intensity variation was adjusted to a level consistent with the electrically active thickness obtained from the off-axis results. The resulting fitted depletion widths and charge densities are

shown in Fig. 4, plotted as a function of electrically active thickness. The in-line results show smaller scatter than the off-axis results arising from a higher sampling density and improved sensitivity to higher frequency potential variations across the *p-n* junction. The plots in Fig. 4 provide a value of 100 nm for the depletion width in an unbiased sample, with a charge density of 3×10^{17} cm^{-3}. The equivalent values obtained from the biased sample provide a charge density of 6.5×10^{17} cm^{-3}, suggesting that the electrical bias applied may 'reactivate' some of the charge in the sample that has been passivated by sample preparation.

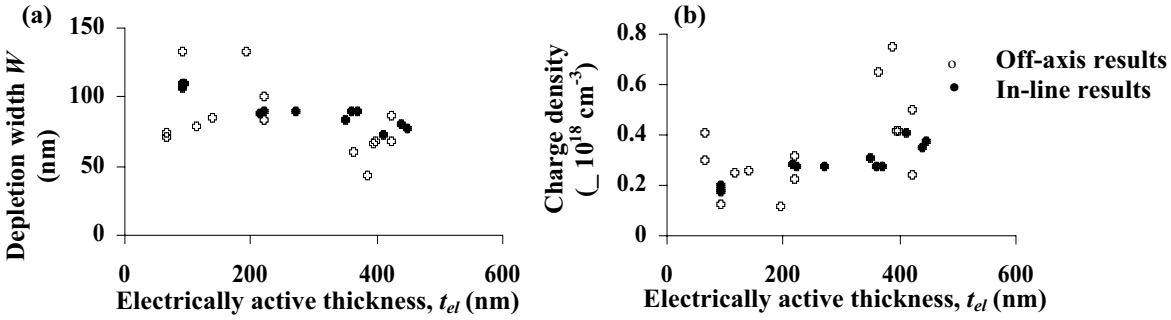

Fig. 4: (a) Fitted depletion width and (b) charge density in the depletion region as a function of electrically active thickness for unbiased off-axis and in-line results obtained from FIB-prepared membranes.

Thickness measurements obtained from the reconstructed amplitude image and using CBED revealed the presence of 60-nm-thick amorphous material on the surfaces. This could arise from sample preparation in the focused ion beam workstation as the ion beam is known to generate damaged surface layers with significant Ga ion implantation (McCaffrey et al 2001). A layered structure for the internal electrostatic potential distribution in an FIB-prepared TEM membrane can be inferred by compiling all biased and unbiased experimental results; this is illustrated in Fig.5.

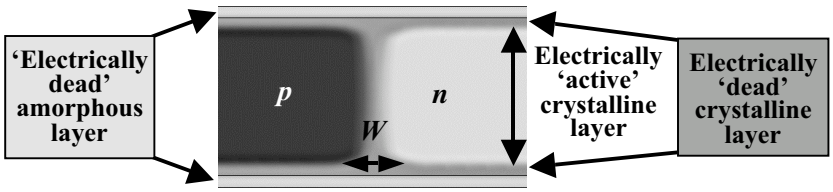

Fig. 5: Schematic diagram of the proposed layered structure present in a FIB prepared Si membrane deduced from off-axis and in-line electron holography results.

4. CONCLUSIONS

Off-axis and in-line electron holography experiments have revealed the internal electrostatic potential distribution in FIB-prepared membranes of a Si *p-n* junction. Electrical biasing experiments have shown that crystalline, electrically dead material is present on the membranes. The unbiased experiments, in conjunction with simulations, have revealed a variation in depletion width with depth in the membrane. Matching simulations with the experimental results has allowed a quantitative analysis of the junction properties to be carried out.

ACKNOWLEDGEMENTS

The authors would like to thank Dr. R. F. Broom for his assistance and advice, Philips Research Laboratories (Eindhoven) for providing the Si device and Newnham College, the Royal Society and EPSRC for financial support.

REFERENCES

Gajdardziska-Josifovska M and McCartney M R 1994 Ultramicroscopy **53**, 283

McCaffrey J P, Phaneuf M W and Madsen L D 2001 Ultramicroscopy **87**, 97

Rau W D, Schwander P, Baumann F H, Hoppner W and Ourmazd A 1999 Phys. Rev. Lett., **82,** 12, 2614

Saxton W O, Pitt T J and Horner M 1979 Ultramicrosocopy **4**, 343

Twitchett A C, Dunin-Borkowski R E and Midgley P A 2002 Phys. Rev. Lett. **88**, 238302